

Nonlinear Vibration Behavior of the Duffing Equation

M475 - Spring 2016

Gary Collins - Cullen Briere - Sam Rose

May 8, 2016

1. Introduction

The Duffing Equation is a mathematical representation of a Duffing oscillator – a damped, driven, nonlinear mass-spring system. By studying the behavior of the Duffing Equation with various parameters, we are able to make physical predictions on how the system will behave.

We discuss how the boundedness of the system can be determined for the unforced, undamped scenario by examining its parameters, particularly the ratio of the nonlinear and linear coefficients in section 3. Additionally, we approximated the steady-state solution of a damped and forced system with negative linear and positive nonlinear stiffness subjected to a constant force. Under the assumption that the ratio of the linear and nonlinear coefficients is sufficiently small, the method yields a strong approximation in section 4. We also examined and discussed the jump phenomena that occurs in our analytical analysis in section 5.1. Lastly, through nondimensionalization of the Duffing Equation, we found an analytical solution for the steady-state response in an underdamped system in section 5.2. Numerical verifications of each subject are provided at the end of the report in section 7.

2. Problem Statement and Assumptions

Consider a forced mass spring-damped system as presented in figure 2.1,

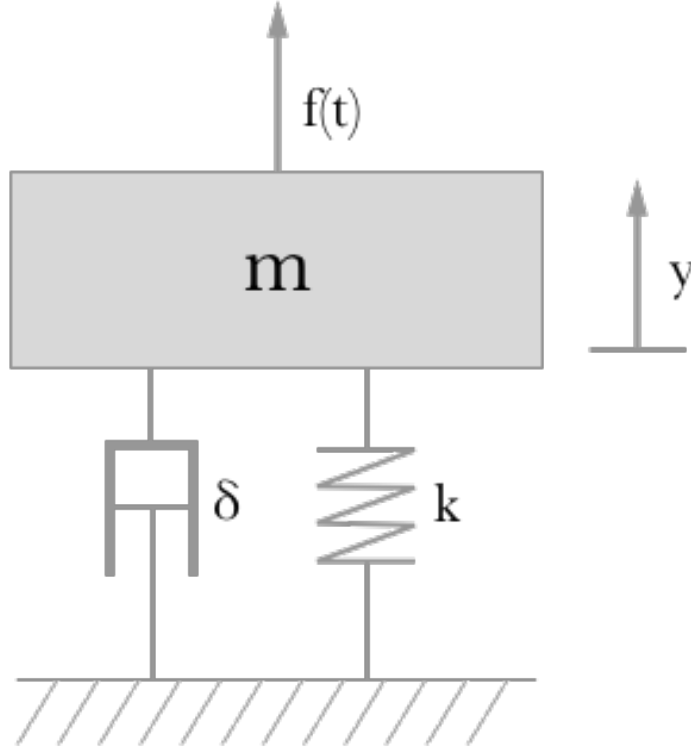


Figure 2.1: A damped mass-spring system with a driving force of $f(t)$

where m is the mass, c is the damping coefficient, k is the spring coefficient, and $F(t)$ is some force dependent on time. The force created by the damper is linearly dependent on the velocity of the mass, $F_d(t) = -c \cdot v = -c \cdot \dot{x}(t)$, and the force of the spring is linearly dependent on the systems displacement from its natural equilibrium, $F_s(t) = -k \cdot (x(t) - x_e(t))$. Following Newtons Second Law of Motion and setting the natural equilibrium of the system to be 0 yields,

$$m\ddot{x}(t) = \sum F = F(t) - F_s(t) - F_d(t) \quad (2.1)$$

$$\implies m\ddot{x}(t) + c\dot{x}(t) + kx(t) = F(t) \quad (2.2)$$

Given initial conditions, $x(t_0) = x_0$ and $\dot{x}(t_0) = \dot{x}(t_0) = v_0$, we can find a solution to this ODE by adding the particular solution (also known as the forced response) and homogeneous solution (also known as the free response).

The Duffing Equation is used in modeling nonlinear electrical and mechanical systems. When springs are compressed or stretched beyond their elastic limit, the force created by the spring will no longer be linearly related to its displacement. Commonly, this nonlinear reaction is represented by,

$$F_s(t) = k_1x(t) + k_3x^3(t) \quad (2.3)$$

where k_1 and k_3 are spring constants.

The inclusion of this force along with a sinusoidal forcing function creates the Duffing Equation (also known as the Duffing Oscillator),

$$m\ddot{x}(t) + c\dot{x}(t) + k_1x(t) + k_3x^3(t) = \gamma\cos(\omega t + \phi) \quad (2.4)$$

where m is the mass, c is the damping coefficient, k_1 is the linear spring constant, k_3 is the nonlinear spring constant, γ is the amplitude of the driving force, and ω and ϕ are the frequency and phase angle of the driving force, respectively.

3. Boundedness in Undamped and Unforced Scenarios

Consider an undamped and unforced spring system with a positive linear spring coefficient and a negative nonlinear spring coefficient: $c = 0$, $\gamma = 0$, $k_1 > 0$ and $k_3 < 0$. The resulting dynamical system is,

$$m\ddot{x} + k_1x - k_3x^3 = 0 \quad (3.1)$$

$$\text{or } \ddot{x} = \frac{k_3x^3 - k_1x}{m} \quad (3.2)$$

with initial conditions,

$$x(0) = x_0 \text{ and } \dot{x}(0) = \dot{x}_0 \quad (3.3)$$

The behavior of the system depends highly on its parameters. In response to a displacement, the linear term will try to force the system back to equilibrium while the nonlinear term will try to force the system further away from equilibrium. Furthermore, since $\lim_{x \rightarrow \infty} \frac{k_1x}{k_3x^3} = 0$, the nonlinear term grows at a faster rate than the linear term; thus for large displacement, the system will be forced away from equilibrium at an increasing speed. However, with proper selection of initial conditions and system parameters, the response of the system will remain bounded.

Imagine this system where the nonlinear term, k_3 , is very small. Its effect on the system would be very small compared to the effect of the linear term on the mass. Thus we can approximate the shape of the systems response with,

$$m\ddot{x} + k_1x - k_3x^3 \approx m\ddot{x} + k_1 \text{ for } k_3 \ll k_1 \quad (3.4)$$

The solution to this approximation is a neutrally stable, sinusoidal response 3.1. If k_3 remains relatively small compared to k_1 and the initial conditions, the system will behave nearly sinusoidal. As the parameter k_3 grows larger, the shape of the response becomes less smooth until the value of k_3 is sufficiently large enough to equally oppose the linear springs restoring force at a displacement where the velocity of the mass is zero,

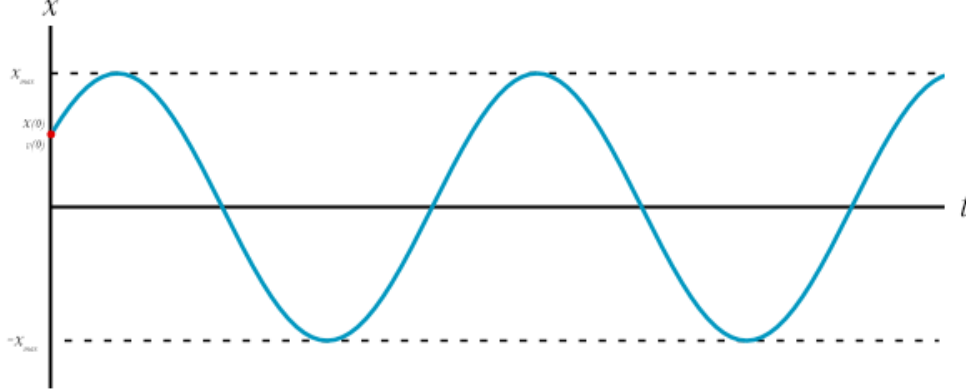


Figure 3.1: A representation of a neutrally stable, sinusoidal response

With these parameter, the mass is at an equilibrium point as,

$$\ddot{x}|_{x_e} = 0 \quad (3.5)$$

$$\ddot{x}|_{x_e} = k_3x_e^3 - k_1x_e = 0 \quad (3.6)$$

If a disturbance were to push the mass beyond x_e then $\ddot{x} = k_3x^3 - k_1x^3 > 0$, thus the mass will accelerate even further away from the equilibrium point. If a disturbance were to push the mass below x_e then $\ddot{x} = k_3x^3 - k_1x^3 < 0$, thus the mass will accelerate even further below the equilibrium point. Thus the equilibrium point x_e is an unstable.

Increasing the value of k_3 even further will cause $k_3x_e^3 > k_1x_e$, and thus at those parameters the mass will accelerate at an increasing rate.

We can ascertain three separate outcomes can occur for an undamped, unforced system depending on the parameters k_1 and k_3 at some displacement x_e where $\dot{x}|_{x_e} = 0$

1. $k_3x_e^3 < k_1x_e \Rightarrow \ddot{x}|_{x_e} = k_3x_e^3 - k_1x_e < 0$, the system remains bounded and resembles sinusoidal behavior.
2. $k_3x_e^3 = k_1x_e \Rightarrow \ddot{x}|_{x_e} = k_3x_e^3 - k_1x_e = 0$, the system will be static at the unstable equilibrium point, x_e .

3. $k_3x_e^3 > k_1x_e \Rightarrow \ddot{x}|_{x_e} = k_3x_e^3 - k_1x_e > 0$, the system will accelerate beyond x_e at an increasing rate.

Consider the first outcome. Since $\dot{x}|_{x_e} = 0$ and $\ddot{x}|_{x_e} < 0$, the mass is at a local maximum. Furthermore, since the system has no forcing function or damping, energy will be conserved and is path independent. Thus, if ever the system returns to this displacement, it will have no kinetic energy as the springs store the total energy of the system; so, the mass can never go beyond this value with these parameters and given initial conditions. Thus the system is bounded above by $x_e = x_{max}$. The value $-x_e$ can be shown to be a lower bound using the same logic. Thus the system is bounded. Furthermore,

$$|k_3|x_{max}^3 - k_1x_{max} < 0 \quad (3.7)$$

$$\Rightarrow k_3x_{max}^3 < k_1x_{max} \quad (3.8)$$

$$\Rightarrow x_{max}^2 < \frac{k_1}{|k_3|} \quad (3.9)$$

The inequality 3.9 holds when the system is bounded and neutrally stable. This is shown numerically later in the paper.

To relate the local maximum, x_{max} , to the initial conditions and parameters of the system, we will look into the total energy of the system. Since there is no forcing function or damping term, the energy of the system is conserved. Thus, the energy of the system at the the initial condition equals the energy of the system at the maximum value,

$$E_{@x_{max}} = E_{t=0} \quad (3.10)$$

$$\iff - \int_0^{x_{max}} F_{spring} dx = \frac{1}{2}m\dot{x}_0^2 - \int_0^{x_0} F_{spring} dx \quad (3.11)$$

$$\iff \frac{1}{2}k_1x_{max}^2 - \frac{1}{4}|k_3|x_{max}^4 = \frac{1}{2}m\dot{x}_0^2 + \frac{1}{4}|k_3|x_0^4 = d \quad (3.12)$$

$$\frac{1}{2}k_1x_{max}^2 - \frac{1}{4}|k_3|x_{max}^4 - d = 0 \quad (3.13)$$

The equation above is a 4th order polynomial of x_{max} , which will produce two real roots. The real roots represent the maximum and minimum values of x or the bounds of the response.

This procedure can be applied to the other inequality relations of k_1 and k_3 .

If $k_1 < 0$ and $k_3 > 0$, then the boundedness condition is $\frac{|k_1|}{k_3} < x_{max}^2$, where

$$\frac{1}{4}k_3x_{max}^4 - \frac{1}{2}|k_1|x_{max}^2 = \frac{1}{2}m\dot{x}_0^2 + \frac{1}{4}k_3x_0^4 - \frac{1}{2}|k_1|x_0^2 \quad (3.14)$$

If $k_1 > 0$ and $k_3 > 0$, then the boundedness condition is $-\frac{k_1}{k_3} < x_{max}^2$, where

$$\frac{1}{4}k_3x_{max}^4 + \frac{1}{2}k_1x_{max}^2 = \frac{1}{2}m\dot{x}_0^2 + \frac{1}{4}k_3x_0^4 + \frac{1}{2}k_1x_0^2 \quad (3.15)$$

If $k_1 < 0$ and $k_3 < 0$, then the boundedness condition is $x_{max}^2 < -\frac{k_1}{k_3}$, where

$$-\frac{1}{4}|k_3|x_{max}^4 - \frac{1}{2}|k_1|x_{max}^2 = \frac{1}{2}m\dot{x}_0^2 - \frac{1}{4}|k_3|x_0^4 - \frac{1}{2}|k_1|x_0^2 \quad (3.16)$$

Notice that the boundedness condition for the two positive spring coefficients is always true, and the boundedness condition for the two negative spring coefficients is always false. Thus, systems with two restoring springs will always be bounded, and a system with two repelling springs will always be unbounded.

4. Approximation under Negative Linear and Positive Nonlinear Stiffnesses

4.1. Approximation of Steady-State Response

Consider a driven mass-damped spring system with negative linear stiffness and positive cubic stiffness. Suppose the system is subjected to a constant force, F_b , while at a stable position of x_d . The force equilibrium equation can then be given by setting the restoring force equal to zero

$$k_1x_d + k_3x_d^3 - F_b = 0 \quad (4.1)$$

where the stable position is given by,

$$x_d = \sqrt{\frac{-k_1}{k_3}} \quad (4.2)$$

If the mass is displaced by δ units from the stable position the restoring force can be expressed as

$$F_r = k_1x_d + k_3x_d^3 - F_b \quad (4.3)$$

Applying Newtons Second Law of Motion to the mass subjected to this restoring force and a damping force proportional to the velocity of the mass, we have the following equation of motion for the system

$$m\ddot{x} + c\dot{x} + k_1x + k_3x^3 = F_b + F_0\cos(\omega t) \quad (4.4)$$

Now, substituting the displacement of the mass with the displacement of the mass δ units from the stable position x_d we have,

$$m\ddot{\delta} + c\dot{\delta} + k_1(x_d + \delta) + k_3(x_d + \delta)^3 = F_b + F_0\cos(\omega t) \quad (4.5)$$

Lastly, subtracting 4.1 from 4.5 yields the following equation of motion for the system,

$$m\ddot{\delta} + c\dot{\delta} + k_l\delta + k_q\delta^2 + k_c\delta^3 = F_0\cos(\omega t) \quad (4.6)$$

where k_1, k_q, k_c denote the linear, quadratic, and cubic stiffness respectively at the stable positions of the system. They can be expressed as follows:

$$k_l = k_1 + 3k_3x_d^2 \quad (4.7)$$

$$k_q = 3k_3x_d \quad (4.8)$$

$$k_c = k_3 \quad (4.9)$$

If δ is much less than x_d , and given that

$$\frac{k_1}{k_3} < \frac{9}{4} \quad (4.10)$$

then the linear force $k_l\delta$ will dominate the system. As a result, we can approximate the equation of motion for the system as,

$$m\ddot{\delta} + c\dot{\delta} + k_l\delta = F_0\cos(\omega t) \quad (4.11)$$

This has solution of

$$\delta = x_0 \sin(\omega t - \phi) \quad (4.12)$$

$$\implies x - x_d = x_0 \sin(\omega t - \phi) \quad (4.13)$$

$$\implies x = x_d + x_0 \sin(\omega t - \phi) \quad (4.14)$$

where,

$$\phi = \tan^{-1}\left(\frac{2\xi\Omega}{1-\Omega^2}\right) \quad (4.15)$$

$$\xi = \frac{c}{2\sqrt{mk_1}} \quad (4.16)$$

$$\Omega = \frac{\omega}{\omega_n} \quad (4.17)$$

$$\omega_n = \frac{1}{2\pi} \sqrt{\frac{k_l}{m}} \quad (4.18)$$

4.2. Boundedness

Recall from section 3 the boundedness condition for the case where $k_1 < 0$ and $k_3 > 0$

$$x_{max}^2 > \frac{|k_1|}{k_3} \quad (4.19)$$

$$\implies x_{max} > \sqrt{\frac{|k_1|}{k_3}} = x_d \quad (4.20)$$

where

$$\frac{1}{4}k_3x_{max}^4 - \frac{1}{2}|k_1|x_{max}^2 = \frac{1}{2}m\dot{x}_0^2 + \frac{1}{4}k_3x_0^4 - \frac{1}{2}|k_1|x_0^2 \quad (4.21)$$

$$\implies \frac{1}{4}k_3x_{max}^4 - \frac{1}{2}|k_1|x_{max}^2 - \frac{1}{2}m\dot{x}_0^2 - \frac{1}{4}k_3x_0^4 + \frac{1}{2}|k_1|x_0^2 = 0 \quad (4.22)$$

A fourth degree polynomial that will produce two real roots that represent the maximum and minimum displacement of the system.

We predicted that not only would we be able to approximate the steady-state response of the system but also analytically show the stability of the system by finding the roots of the polynomial and numerically verifying that $x(t)$ is bounded for all time.

5. Analytical Solution to steady-state Duffing Equation

5.1. “Jump” Phenomena

Recall the Duffing Equation,

$$m\ddot{x}(t) + c\dot{x}(t) + k_1x(t) + k_3x^3(t) = \gamma\cos(\omega t + \phi) \quad (5.1)$$

Analytical solutions for the steady-state response of the Duffing equation can be developed under certain conditions: $k_1 > 0$ and the system is underdamped. First, assume that the form of the solution to the Duffing Equation is expressed as,

$$x(t) = x_1\cos(\omega t) \quad (5.2)$$

Now, for convenience, we will nondimensionalize the Duffing Equation with the following substitutions:

$$X = \frac{k_1x}{\gamma} \quad \text{dimensionless displacement} \quad (5.3)$$

$$X_1 = \frac{k_1x_1}{\gamma} \quad \text{amplitude of assumed solution} \quad (5.4)$$

$$T = \frac{t}{\sqrt{\frac{m}{k_1}}} \quad \text{dimensionless time} \quad (5.5)$$

$$\zeta = \frac{c}{2\sqrt{mk_1}} \quad \text{damping ratio} \quad (5.6)$$

$$k_r = \frac{k_3\gamma^2}{k_1^3} \quad \text{dimensionless nonlinear coefficient} \quad (5.7)$$

$$\Omega = \frac{\omega}{\sqrt{\frac{k_1}{m}}} \quad \text{dimensionless angular frequency} \quad (5.8)$$

With these, equations 5.1 and 5.2 can be transformed into,

$$\frac{d^2X}{dT^2} + 2\zeta\frac{dX}{dT} + X + k_rX^3 = \cos(\Omega T + \phi) \quad (5.9)$$

$$X = X_1\cos(\Omega T) \quad (5.10)$$

Furthermore, we can substitute the trigonometric identity $\cos(\Omega T + \phi) = \cos(\Omega T)\cos(\phi) - \sin(\Omega T)\sin(\phi)$ and the assumed response and its derivatives,

$$\begin{aligned} X_1(1 - \Omega^2)\cos(\Omega T) - 2\zeta(X_1\Omega\sin(\Omega T)) + X_1\cos(\Omega T) + k_r(X_1\cos(\Omega T))^3 \\ = \cos(\Omega T)\cos(\phi) - \sin(\Omega T)\sin(\phi) \end{aligned} \quad (5.11)$$

Multiplying 5.2 by $\sin(\Omega T)$ and $\cos(\Omega T)$ and then integrating the result over one period, we obtain,

$$X_1(1 - \Omega^2) + \frac{3}{4}k_rX_1^3 = \cos(\phi) \quad (5.12)$$

$$2\zeta X_1\Omega = \sin(\phi) \quad (5.13)$$

Substituting these into the Pythagorean trigonometric identity results in,

$$[X_1(1 - \Omega^2) + \frac{3}{4}k_rX_1^3]^2 + [2\zeta X_1\Omega]^2 = 1 \quad (5.14)$$

Expanding 5.9 and substituting $Y = X_1^2$ we obtain,

$$Y^3 + aY^2 + bY + c = 0 \quad (5.15)$$

where

$$a = \frac{8}{3K_r}(1 - \Omega^2) \quad (5.16)$$

$$b = \frac{16}{9k_r^2}[(1 - \Omega^2)^2 + 4\zeta^2\Omega^2] \quad (5.17)$$

$$c = -\frac{16}{9k_r^2} \quad (5.18)$$

The discriminant of 5.10 is defined as,

$$\Delta = 4a^3c - a^2b^2 - 18abc + 4b^3 + 27c^2 \quad (5.19)$$

If $\Delta < 0$, then equation 5.10 has three real roots,

$$Y_1 = \frac{1}{3}[-a + 2\sqrt{a^2 - 3b}\cos(\frac{\psi}{3})] \quad (5.20)$$

$$Y_2 = \frac{1}{3}[-a + 2\sqrt{a^2 - 3b}\cos(\frac{\psi + 2\pi}{3})] \quad (5.21)$$

$$Y_3 = \frac{1}{3}[-a + 2\sqrt{a^2 - 3b}\cos(\frac{\psi + 4\pi}{3})] \quad (5.22)$$

where

$$\psi = \cos^{-1}[\frac{-a^3 + \frac{9}{2}ab - \frac{27}{2}c}{(a^2 - 3b)^{\frac{3}{2}}}] \quad (5.23)$$

Recall that $X_1 = \sqrt{Y}$ and $x_1 = X_1 \frac{\gamma}{k_1}$, thus $x_1 = \sqrt{Y} \frac{\gamma}{k_1}$ is the amplitude of our steady-state solution.

Note that the nondimensional steady-state amplitude is a function of k_r , ζ , and Ω . Below is a plot of the nondimensional steady-state amplitude versus the frequency ratio,

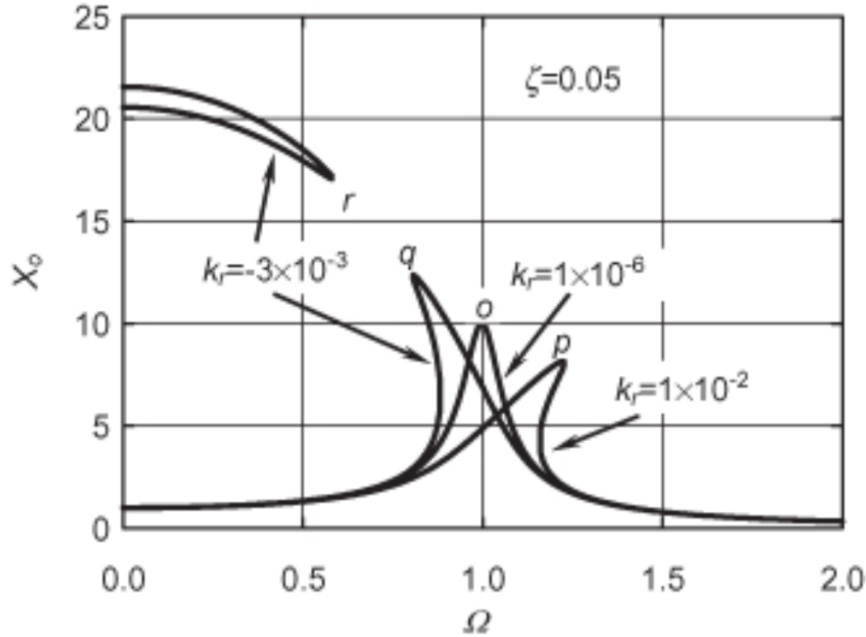


Figure 5.1: Nondimensional steady-state amplitude vs the frequency ratio. [1]

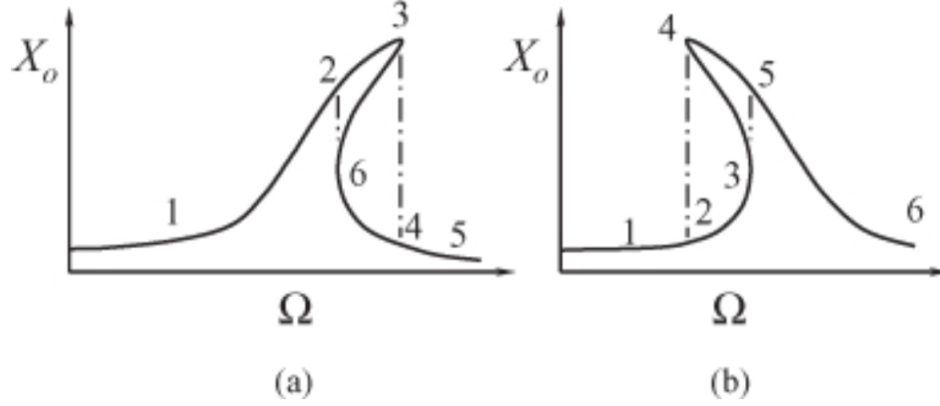


Figure 5.2: *Jump phenomena of nonlinear oscillator [1]*

Experimental data demonstrate the jump phenomena of nonlinear systems. For a hardening spring ($k_r > 0$), 5.2a, as Ω sweeps up, X_1 follows the path 1-2-3-4-5, with the amplitude jumping down from 3 to 4; however, when Ω is swept down, the path followed is 5-4-6-2-1, with the amplitude jumping up from 6 to 2. Experimental data of the path from 3-6 is not obtainable in experiments and is an unstable solution.

For softening springs ($k_r < 0$), 5.2b, X_1 follows the path 1-2-4-5-6 as is swept up, jumping from 2 to 4; and when Ω is swept down, the path followed is 6-5-3-2-1, jumping from 5 to 3.

For a nearly linear spring, the system does not demonstrate the jump phenomena.

5.2. Analytical Solution of Stead-State Response

The maximum amplitude and its corresponding angular frequency can be obtained analytically. These values represent points 3 and 4 on figure 5.2a and 5.2b, respectively. Rearranging equation 5.15 to be in terms of $(1 - \Omega^2)$ obtains,

$$(1 - \Omega^2)^2 + \left(\frac{3K_r}{2}Y^2 - 4\zeta^2Y\right)(1 - \Omega^2) + \frac{9k_r^2}{16}Y^3 + 4\zeta^2Y - 1 = 0 \quad (5.24)$$

whose solution is found using the quadratic equation,

$$(1 - \Omega^2)^2 = \frac{1}{2Y} \left[-\left(\frac{3k_r}{2}Y^2 - 4\zeta^2Y\right) \pm \sqrt{D_1} \right] \quad (5.25)$$

where $D_1 = \left(\frac{3k_r}{2}Y^2 - 4\zeta^2Y^2\right) - 4Y\left(\frac{9k_r^2}{16}Y^3 + 4\zeta^2Y - 1\right)$, is the discriminant of the equation. $D_1 = 0$ corresponds with the maximum value of Y . Rearranging equation 5.25 with $D_1 = 0$, gives

$$-4Y_m[3k_r\zeta^2Y_m^2 + 4\zeta^2(1 - \zeta^2)Y_m - 1] = 0 \quad (5.26)$$

where Y_m is the maximum value. This yields two solutions for Y_m ,

$$Y_{m1} = \frac{2}{3} \frac{1 - \zeta^2}{k_r} [-1 + \sqrt{1 + \frac{3k_r}{4\zeta^2(1 - \zeta^2)}}] \quad (5.27)$$

$$Y_{m2} = \frac{2}{3} \frac{1 - \zeta^2}{k_r} [-1 - \sqrt{1 + \frac{3k_r}{4\zeta^2(1 - \zeta^2)}}] \quad (5.28)$$

Of the two, experimental data shows that Y_{m1} can be achieved, so the remainder will be focused on it.

The using the identity, $X_0 = Y_{m1}$ and rearranging equation 5.27 and substituting Y_{m1} , we obtain,

$$X_{1m} = \sqrt{\frac{2}{3} \frac{1 - \zeta^2}{k_r} [-1 + \sqrt{1 + \frac{3k_r}{4\zeta^2(1 - \zeta^2)}}]} \quad (5.29)$$

$$\Omega_m = \sqrt{1 - 2\zeta^2 - \frac{1 - \zeta^2}{2} [-1 + \sqrt{1 + \frac{3k_r}{4\zeta^2(1 - \zeta^2)}}]} \quad (5.30)$$

For cases where the system is only slightly damped ($\zeta \ll 1$), the system can be approximated as,

$$X_{1m} \approx \sqrt{\frac{2}{3k_r} (-1 + \sqrt{1 + \frac{3k_r}{4\zeta^2}})} \quad (5.31)$$

$$\Omega_m \approx \sqrt{1 - 2\zeta^2 - \frac{1}{2} [1 - \sqrt{1 + \frac{3k_r}{4\zeta^2}}]} \quad (5.32)$$

The objective of our experiment is to solve the Duffing Equation using various well-know numerical methods, then compare the results of each model to determine which scheme simulates the nonlinear oscillator most accurately.

We will be observing several cases for each method which to test the Duffing Equation. These cases have various assumptions, as described more in depth below, and stimulate radically different responses. The only parameter that remains consistent throughout our testable cases is the mass, where $m = 1$. One other assumption that must be made is that the system is underdamped. By assuming an underdamped system, we will obtain more interesting results by allowing the system to oscillate more freely and with greater dynamics.

6. Methods

Using various numerical schemes that we have programmatically implemented, we can simulate the behavior of the oscillator system. For each scheme, the process is fairly straightforward: select a scheme to test, execute the scheme with the parameters for each case, plot results (time vs distance and the phase plot), save and document for later comparison after all results have been obtained.

Euler's method, graphically speaking, draws a line from the initial point of the solution to be solved for to its next time step value with the same slope. The endpoint of that line is then the initial point of the next line to be drawn. Euler's method is a first order accurate scheme for solving initial value problems for Ordinary Differential Equations. A great advantage to this method is that it is robust and explicit in its forward form. One issue with the forward form is the fact that it is first order accurate; a higher number of iterations is required compared to other complex solvers. The backwards form, although suffering economically by being an implicit scheme, has greater stability than its forward counterpart.

The Classical Runge-Kutta Method is a method that judiciously uses four approximations of the slope at each time step in order to extrapolate the solution at the future time step. This method applies to first order ordinary differential equations, however, by using reduction of order it can be applied to higher order differential equations. An advantage of this method is that it does not require explicit evaluation of the derivatives, but rather uses a linear combination of values of the differential equation to approximate the solution.

The Velocity Verlet method is a symplectic integrator that solves any second order ordinary differential equation, but was inspired by Newton's Second Law of Motion. This method is advantageous to others as it has better stability on large time intervals.

Using each of the above methods, we numerically solved the system with specified parameters and then compared the solutions on a single component graph (time v.s. displacement) and the Verlet solution on a phase plane (displacement v.s. velocity) for analysis. During each case, we compared the behavior of our numerical solutions with the theoretical prediction for the solutions behavior. Since the Verlet method has better stability over long time intervals, we used our Verlet scheme as the accepted numerical solution. To ensure only valid solutions would be plotted, we implemented a maximum residual check so that only the methods whose maximum error is less than two times the maximum Verlet value. In order to further improve our results from the Verlet scheme, if c is not equal to zero then a rootfinder is implemented to increase the efficiency of finding the solution as the value of the velocity and acceleration at the next time step are coupled.

7. Solution / Results

7.1. Boundedness Condition for Undamped/Unforced Systems

In this case, the damping ratio is zero and there is no forcing function. Thus, the relationships established in section 3 can be applied to determine the stability of the system. First, we shall

numerically verify our procedure with a simplified case. Set $m = 1, c = 0, k_1 > 0$, and $k_3 < 0$ with the initial conditions $x_0 = 2$ and $v_0 = 0$. From the equation $\frac{1}{32}k_1x_{max}^2 - \frac{1}{4}k_3x_{max}^4 = \frac{1}{2}m\dot{x}_0^2 + \frac{1}{2}k_1x_0^2 - \frac{1}{4}|k_3|x_0^4$, we can see that $x_{max} = x_0 = 2$. The boundedness condition then is,

$$x_{max}^2 = 4 < \frac{k_1}{|k_3|} \quad (7.1)$$

$$\iff 4|k_3| < k_1 \quad (7.2)$$

Consider $k_3 = -1$ and $k_1 = 4, k_1 = 3.9$, and $k_1 = 4.1$.

For $k_1 = 4$:

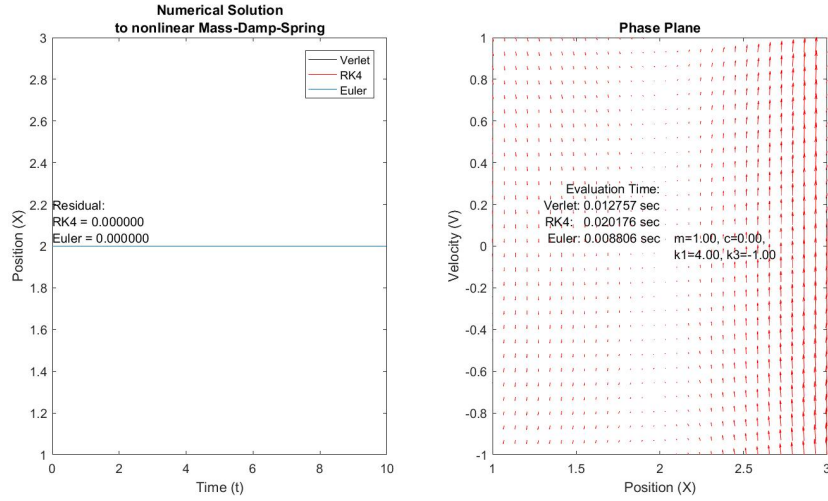


Figure 7.1

This system represents one where the system is at an unstable equilibrium as seen by the directional map. If the system were to be perturbed down, then the system would enter a steady-state oscillation. If it were to be perturbed upward, it would accelerate toward infinity and thus be unbounded.

For $k_1 = 3.9$:

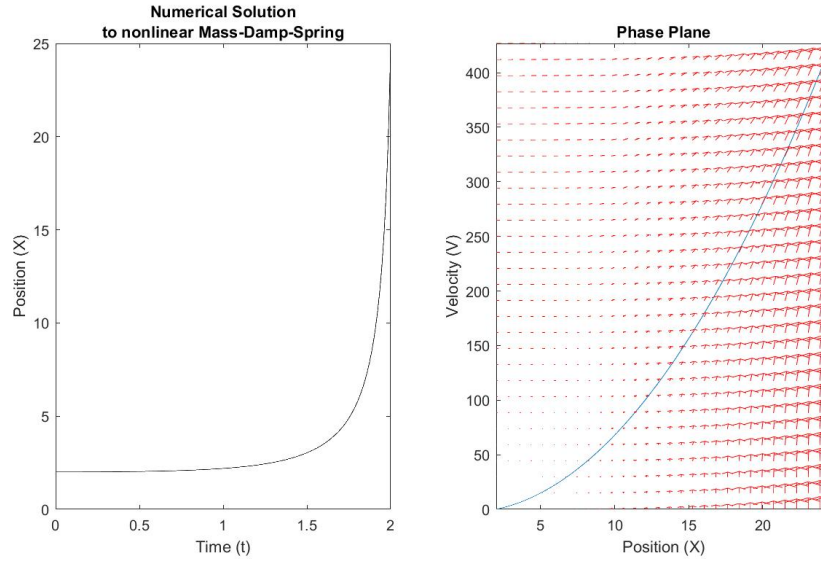


Figure 7.2

As our theory predicts, the system becomes unbounded and accelerates towards infinity since the boundedness condition was not met.

For $k_1 = 4.1$:

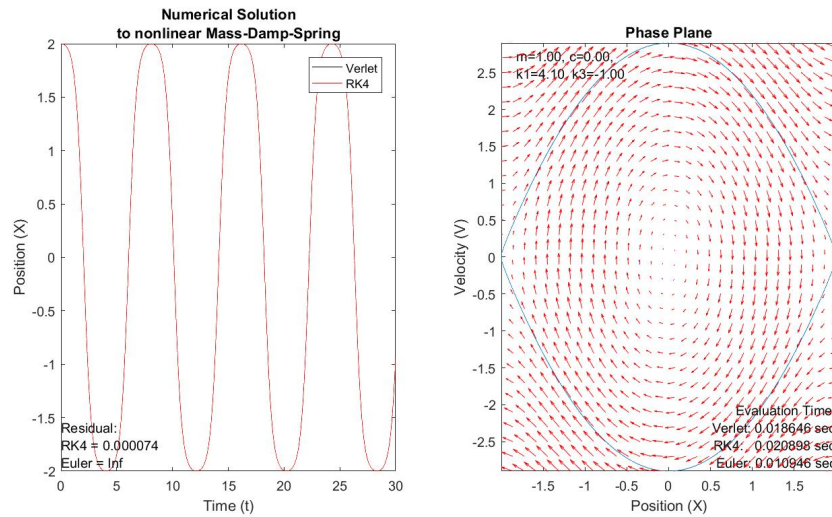


Figure 7.3

Matching our theory's prediction, the motion of the mass closely matches a sinusoidal wave and remains bounded. Under the solutions to the roots of the polynomial given earlier. However, notice that the shape of the phase plane is not exactly circular. This indicates the movement of the mass not being exactly sinusoidal.

In order to obtain more sinusoidal behavior, the ratio of $\frac{k_1}{k_3}$ should be increased, as the larger k_1 is in respect to k_3 , the effect of more dominant the linear term on the system is and the closer the system matches the behavior of

$$m\ddot{x} = -k_1x, x(0) = x_0, \text{ and } \dot{x}(0) = 0 \quad (7.3)$$

whose solution is

$$x(t) = x_0 \cos \sqrt{\frac{k_1}{m}} t \quad (7.4)$$

Here is an example to verify this convergence.

$k_1 = 20$:

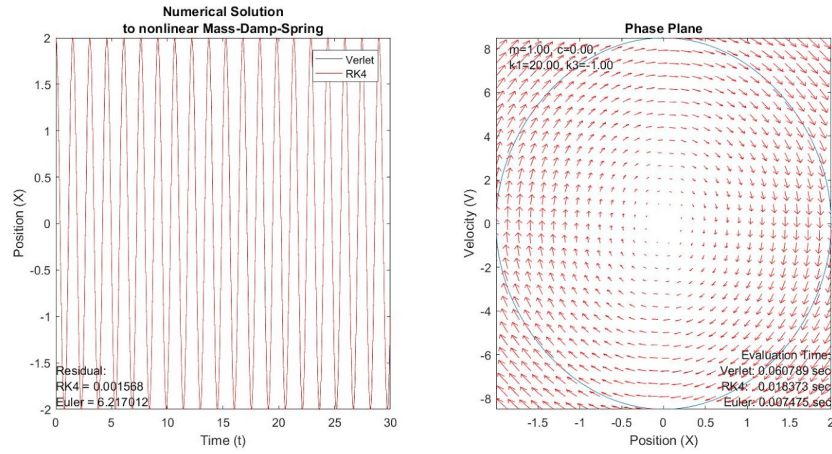


Figure 7.4

Now we shall consider the undamped/unforced scenario with parameters $m = 1, k_1 = -1, k_3 = 1, x_0 = 1, v_0 = 1$.

The solution to,

$$\frac{1}{4}k_3x_{max}^4 - \frac{1}{2}|k_1|x_{max}^2 = \frac{1}{2}m\dot{x}_0^4 - \frac{1}{2}|k_1|x_0^2 \quad (7.5)$$

$$\Rightarrow \frac{1}{4}x_{max}^4 - \frac{1}{2}x_{max}^2 = \frac{1}{4} \quad (7.6)$$

is $x_{1,2} = \pm\sqrt{1+\sqrt{2}} \approx \pm 1.553773974$. Thus the solution is stable and bounded by $x_{1,2}$, as $\frac{|k_1|}{k_3} = 1 < x_{1,2}^2 = 2.414213562$.

This is numerically verified:

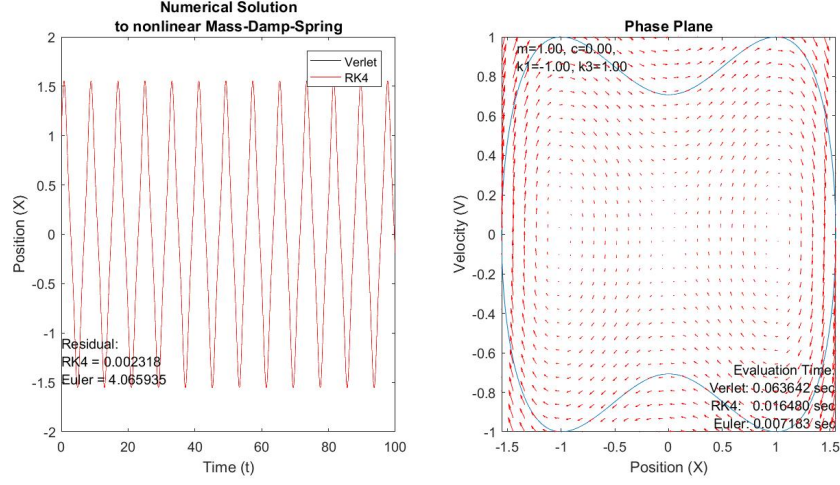


Figure 7.5

Notice that the phase plane is not circular at all, indicating a non-sinusoidal behavior in the solution. This is due to the system now approaching the solution to,

$$m\ddot{x} = -k_3x^3, \quad x(0) = x_0, \text{ and } \dot{x}(0) = \dot{x}_0 \quad (7.7)$$

which is

$$x(t) = \pm i \cdot 2^{\frac{1}{4}} \cdot \sqrt{-\frac{\sqrt{k}}{\sqrt{C_1}}} \sqrt{C_1} \cdot sn\left[\frac{1}{\sqrt{2}} \sqrt{\sqrt{2kC_1}t^2 + 2\sqrt{2kC_1}C_2t + \sqrt{2kC_1}C_2^2}, -1\right] \quad (7.8)$$

where C_1 and C_2 are constants and $sn[*,*]$ is the Jacobi Elliptic Sine Function.

7.2. Evaluation of Approximation of Steady-State Response for Negative Linear and Positive Nonlinear Stiffnesses

In this case, the driven mass-damped system has a negative linear stiffness and a positive cubic stiffness. Recall that if we initially displace the system by δ units from a state of equilibrium and the condition,

$$\frac{k_1}{k_3} < \frac{9}{4} \quad (7.9)$$

is satisfied then the equation of motion of the system is

$$m\ddot{\delta} + c\dot{\delta} + k_l\delta = F_0\cos(\omega t) \quad (7.10)$$

where $k_l = k_1 + 3k_3x_d^2$ denotes the linear stiffness at the stable positions of the system, which has solution

$$\delta = x_0\sin(\omega t - \phi) \quad (7.11)$$

$$\implies x - x_d = x_0\sin(\omega t - \phi) \quad (7.12)$$

$$\implies x = x_d + x_0\sin(\omega t - \phi) \quad (7.13)$$

where,

$$\phi = \tan^{-1}\left(\frac{2\xi\Omega}{1 - \Omega^2}\right) \quad (7.14)$$

$$\xi = \frac{c}{2\sqrt{mk_l}} \quad (7.15)$$

$$\Omega = \frac{\omega}{\omega_n} \quad (7.16)$$

$$\omega_n = \frac{1}{2\pi} \sqrt{\frac{k_l}{m}} \quad (7.17)$$

Furthermore, we discussed the boundedness of the solution $x(t)$ for all time t which shows stability of the solution. We now explore these topics further.

Consider the underdamped system,

$$m = 1, c = 0.2, k_1 = -10, k_3 = .4, F_0 = 0.03, \omega = 1; \quad x_0 = 0.01, \dot{x}_0 = 0. \quad (7.18)$$

Suppose that the mass is at a stable position and that it is not subjected to a constant force. By 4.2 we obtain $x_d = \pm 5$ which yields stiffnesses

$$k_l = 20 \quad (7.19)$$

$$k_q = \pm 6 \quad (7.20)$$

$$k_c = 0.4 \quad (7.21)$$

reducing the nondimensional frequency Ω and damping ratio ξ to,

$$\Omega = 2\sqrt{10} \ , \ \xi = \frac{\sqrt{5}}{100} \quad (7.22)$$

Recall the fourth degree polynomial

$$\frac{1}{4}k_3x_{max}^4 - \frac{1}{2}|k_1|x_{max}^2 - \frac{1}{2}m\dot{x}_0^2 - \frac{1}{4}k_3x_0^4 + \frac{1}{2}|k_1|x_0^2 = 0 \quad (7.23)$$

in which we obtain the maximum displacement of the system. Substituting the parameters

$$m = 1, c = 0.2, k_1 = -10, k_3 = 0.4, F_0 = 0.03, \omega = 1; x_0 = 0.01, \dot{x}_0 = 0 \quad (7.24)$$

into 7.23 and solving for x_{max} we obtain the real roots,

$$x_{max} = 5\sqrt{2}, \ x_{min} = -5\sqrt{2} \quad (7.25)$$

which satisfy the boundedness condition

$$x_{max} = 5\sqrt{2} > 5 = x_d \quad (7.26)$$

Thus since this holds true, we predict that the total response will be bounded for all time and thus the solution $x(t)$ will be stable. However, since

$$\lim_{t \rightarrow \infty} x(t) \approx x_d + x_0 \sin(\omega t - \phi) \neq 0$$

we know that this solution will not be asymptotically stable and so it will decay to a state of neutral stability.

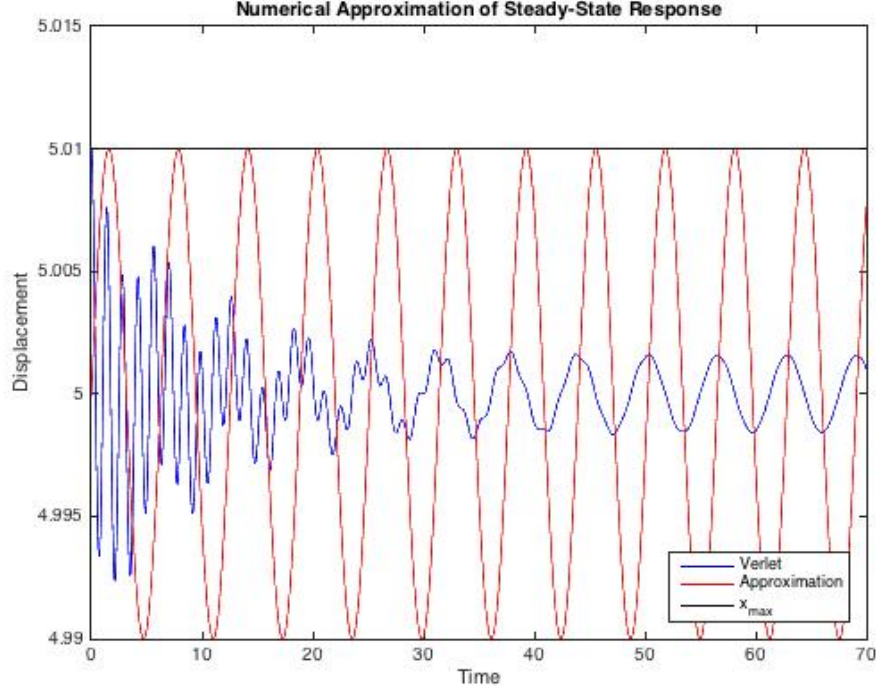


Figure 7.6

As figure 7.6 shows, our approximation method captures the steady-state response. Notice the nonlinear behavior of the solution inevitably dissipates due to the condition $\frac{k_1}{k_3} < \frac{9}{4}$

After 6000 time steps our Verlet Scheme produced a steady-state response for $x(t)$ of which our approximation had a low relative error of 0.13%

Furthermore, we see that the boundedness condition $x_{max} = 5\sqrt{2} > 5 = x_d$ is satisfied and thus the solution $x(t)$ decays to a state of neutral stability, verifying our prediction.

Thus, due to the low relative error of our approximation to the solution, we may conclude that our approximation is consistent to the steady-state response to the Duffing Equation.

7.3. The Jump Phenomena and Analytical Solution to Steady-State Response

Consider the system $m = 1, \delta = 0.1, k_1 = 1, k_3 = 1 \times 10^{-2}, \gamma = 1$, and $0 < \omega < 2$. Thus, $\zeta = 0.05$ and $k_r = 0.01$.

Applying the methods used to obtain 5.20 and plotting the nondimensional amplitudes for this case versus the nondimensional frequency obtains,

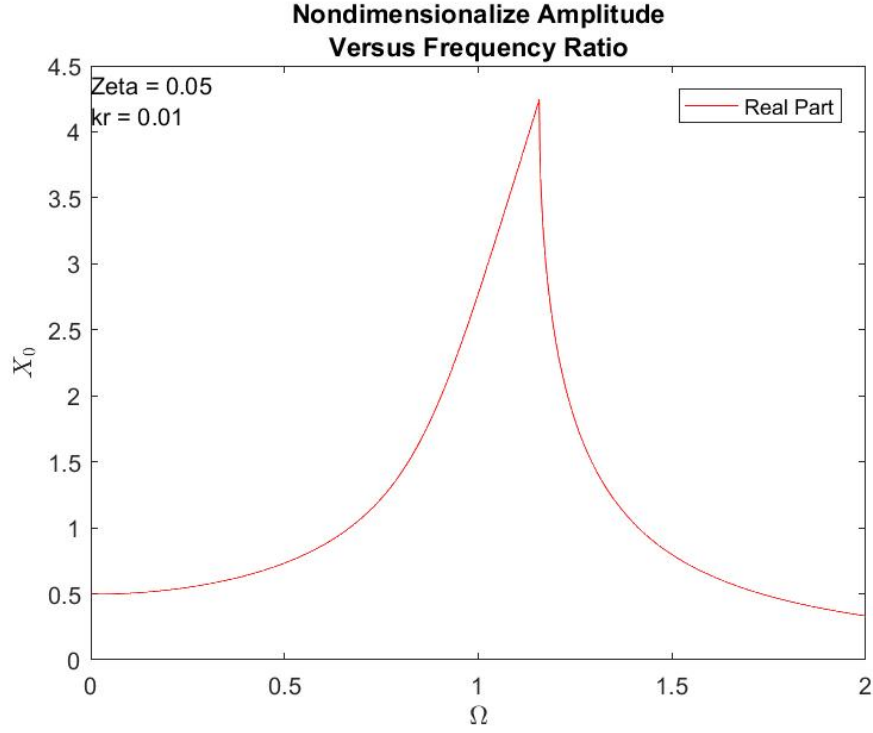


Figure 7.7

The amplitude ratio here behaves like 5.2a and jumps amplitude.

The nondimensional angular frequency associated with peak value of the nondimensional amplitude is $\Omega \approx 1.1577$. Since the value of $m = 1$, $k_1 = 1$, and $\gamma = 1$, dimensionalized angular frequency associated with the maximum steady-state response amplitude is $\omega_m = 1.1577$. In order to show the validity of this analysis and the effects of the jump, we used the Verlet scheme to numerically solve this case with $\omega = \omega_m$ and with $\omega = 1.01 \cdot \omega_m$, a 1% offset. These results were plotted on equal axes.

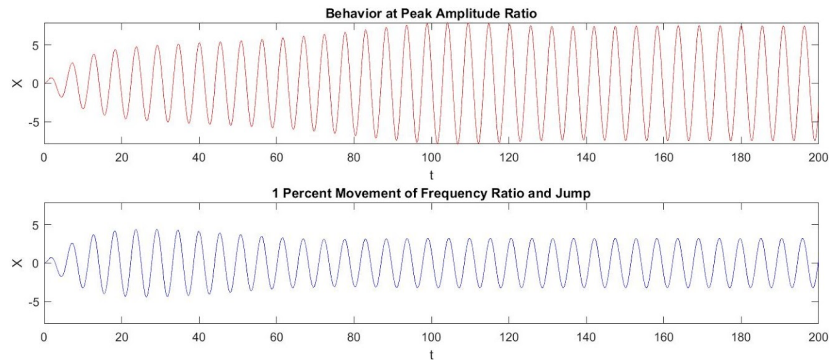


Figure 7.8

As shown above, a 1% change in the angular frequency changes the systems response from a

steady-state response amplitude of ~ 7.5 to ~ 3.2 . This slight change in parameters affecting the system behavior speaks to the sensitivity of the system to the frequency of the forcing function.

The analytical solution and a numerical solution made by using Verlet's Scheme are plotted below.

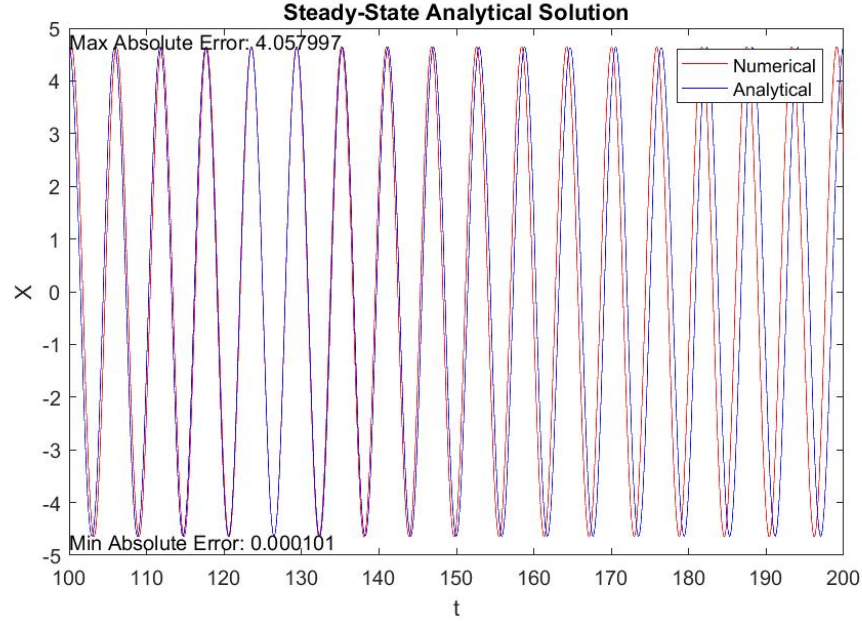


Figure 7.9

The maximum absolute error was quite high; however, this is due to the slight differences in angular frequencies that causes the two solutions to go in and out of phase. The two solutions amplitudes were quite close: Numerical Solution Amplitude ~ 4.648058 and Analytical Solution Amplitude ~ 4.636655 . The main cause of error in the numerical solution would come from discretization and round-off error, while error in the analytical solution would come from round-off and error magnification due to the complicated arithmetic involved in the calculation of the solution constants.

8. Discussion and Conclusions

The Duffing Equation is a vital nonlinear differential equation used to model nonlinear mechanical and electrical systems. Proper numerical analysis is needed to capture its behavior as it is highly sensitive to the parameter values and there is no general analytical solution. This paper developed boundedness conditions for the undamped and unforced systems; evaluated an approximate solution to the steady-state response of a system under negative linear and positive nonlinear stiffness; and explored the jump phenomena, its effects on the response amplitude, and an analytical solution to certain systems.

Although a comparison of schemes used was not mentioned earlier, the results from Section 1 of the results gives insight into their strengths. Verlet's results were the most consistent on changing

time step sizes. As the step size was decreased, Verlets results only slightly changed, while Euler and Classical Runge-Kutta slowly converged towards Verlet. The residual between Euler and Verlet was significantly larger than that of Runge-Kutta and Verlet — in some cases, Euler even diverged. These residuals increase with increased time scales; however, Verlet remained consistent. This is expected as Verlet is a symplectic scheme, having greater stability for long time scales. Euler was the fastest of the schemes. When there is no damping, Runge-Kutta was only slightly slower than Euler, with Verlet being almost taking twice as long. However, the longer evaluation time is still relatively short, so the added precision is worth the decreased efficiency. This changes, however, when there is damping, as Verlets evaluation time becomes 200 times longer than it was without damping. This is due to the need of the Verlet scheme to solve a system at each iteration as two computed values are coupled. Here, Runge-Kutta may be the better choice of the two, although having less accuracy, offering a quicker evaluation of the system.

References

[1] Ki Bang Lee. *Principles of Microelectromechanical Systems*. 2010.

A. Appendix

A.1. Code

A.1.1. Verlet, Euler, and RK4 to numerically solve cases

```
function M475GroupProject(a,b,N,m,c,k1,k3,A,w,x0,v0)
%using Verlet, Euler, and RK4 to numerically solve the case. Also capturing
%time of evaluation for each scheme and residual of the the Euler and RK in
%comparison to Verlet
close all
if c~=0
    tEval1=tic;
    [t,xVer,vVer]=M475VerletVelocity(a,b,N,m,c,k1,k3,A,w,x0,v0);
    tEvalVerlet=toc(tEval1);
else
    tEval1=tic;
    [t,xVer,vVer]=M475VerletNoVelocity(a,b,N,m,c,k1,k3,A,w,x0,v0);
    tEvalVerlet=toc(tEval1);
end %checks the for damping, no velcoity verlet is much faster
tEval2=tic;
[t,xRK,vRK]=M475RK4(a,b,N,m,c,k1,k3,A,w,x0,v0);
tEvalRK4=toc(tEval2);

tEval3=tic;
[t,xEu,vEu]=M475DuffingEuler(a,b,N,m,c,k1,k3,A,w,x0,v0);
tEvalEuler=toc(tEval3);

ResVerRK=max(abs(xRK-xVer));
```



```

ResVerEu=max(abs(xEu-xVer));

%% plotting
close all
subplot(1,2,1)
plot(t,xVer,'k')
if ResVerRK<2*max(xVer) %if the difference is too great, it won't be plotted
    % to keep good resolution of Verlet resolution
    hold on
    plot(t,xRK,'r-');
    if ResVerEu==2*max(xVer)
        hold on
        plot(t,xEu);
        legend('Verlet','RK4','Euler');
    else
        legend('Verlet','RK4');
    end
elseif ResVerEu<2*max(xVer)
    hold on
    plot(t,xEu);
    legend('Verlet','Euler');
else
    legend('Verlet');
end

title(sprintf('Numerical Solution\nto nonlinear Mass-Damp-Spring'));
xlabel('Time (t)');
ylabel('Position (X)');
text(min(t),min(xVer),sprintf('Residual:\nRK4 = %f\nEuler = %f',ResVerRK,ResVerEu),...
    'HorizontalAlignment','left','VerticalAlignment','bottom')
%% Plotting phase plane and directional map
subplot(1,2,2)
plot(xVer,vVer);
title('Phase Plane');
xlabel('Position (X)');
ylabel('Velocity (V)');
text(min(xVer),max(vVer)-.1*max(vVer), sprintf('    m=%.2f, c=%.2f,\n    k1=%.2f, k3=%
    .2f',m,c,k1,k3));
text(max(xVer),min(vVer),sprintf('Evaluation Time:\t\tVerlet: \t%f sec\t\tRK4: \t%f
    sec\t\tEuler: \t%f sec\t',...
    tEvalVerlet,tEvalRK4,tEvalEuler),'HorizontalAlignment','right','VerticalAlignment'
    ,'bottom');
hold on
[xx,yy,uu,vv,y1,y2]=PhasePlanes(a,b,N,m,c,k1,k3,A,w,x0,v0,[min(xVer) max(xVer)], [min(
    vVer) max(vVer)]);
quiver(xx,yy,uu,vv,'r')
xlim([min(y1) max(y1)]);
ylim([min(y2) max(y2)]);
end

```

A.1.2. Euler scheme to numerically solve cases

```

function [t,x,u]=M475DuffingEuler(a,b,N,m,c,k1,k3,A,w,x0,v0)

dt=(b-a)/N;
x(1)=x0;

```

```

u(1)=v0;
t(1)=a; %initialize

for i=1:N-1 %main loop and euler scheme
    t(i+1)=a+i*dt;
    x(i+1)=x(i)+dt*u(i);
    u(i+1)=u(i)+dt*V(t(i),x(i),u(i),m,c,k1,k3,A,w);
end
end

```

A.1.3. Verlet scheme to numerically solve cases with velocity

```

%% M475VerletVelocity.m
% Gary Collins; 15 March 2016
% for plotting the nonlinear mass spring system.
% m*x'' + c*x' + k1*x + k3*x^3 = A*cosine(w*t)
function [t,x,v]=M475VerletVelocity(a,b,N,m,c,k1,k3,A,w,x0,v0)
% initializing variables
dt=(b-a)/N;
x(1)=x0; %position
v(1)=v0; %velocity
t=a; %time
acc(1)=V(t,x(1),v(1),m,c,k1,k3,A,w); %acceleration
%% main loop
for i=1:N-1
    x(i+1)=x(i)+v(i)*dt+.5*acc(i)*dt^2;
    v2=v(i)+.5*acc(i)*dt; % corrector velocity
    t(i+1)=a+i*dt; %advances time
    if abs(v2)>=1E8
        break
    end
    % the next line is used to find the appropiate velocity and acceleration
    % at the next time step as the procedure described in the verlet
    % velocity scheme assumes that the force (thereby acceleration) is not
    % dependent on velocity. However, as they are dependent on each other,
    % i used a root finded on the function Residual. Residual is described
    % below.
    v(i+1)=fzero(@(v) (Residual(dt,t(i+1),x(i+1),v,v2,m,c,k1,k3,A,w)),v2);
    acc(i+1)=V(t(i+1),x(i+1),v(i+1),m,c,k1,k3,A,w);
end
end

%% Residual
% needed to find acceleration and velocity at i+1 time step. It was made by
% taking the last two steps of the verlet velocity scheme, subistuting the
% third step into the fourth and substracting v(t+dt) from both sides.
function res=Residual(dt,t,x,v,v2,m,c,k1,k3,A,w)
res=v2+.5*V(t,x,v,m,c,k1,k3,A,w)*dt-v;
end

```

A.1.4. Verlet scheme to numerically solve cases without velocity

```

%% M475VerletVelocity.m
% Gary Collins; 15 March 2016

```

```

% for plotting the nonlinear mass spring system.
% m*x'' + c*x' + k1*x + k3*x^3 = A*cosine(w*t)
function [t,x,v]=M475VerletNoVelocity(a,b,N,m,c,k1,k3,A,w,x0,v0)

% initializing variables
dt=(b-a)/N;
x(1)=x0; %position
v(1)=v0; %velocity
t=a; %time
acc(1)=V(t,x(1),v(1),m,c,k1,k3,A,w); %acceleration
%% main loop
for i=1:N-1
    x(i+1)=x(i)+v(i)*dt+.5*acc(i)*dt^2;
    v2=v(i)+.5*acc(i)*dt; % corrector velocity
    t(i+1)=a+i*dt; %advances time
    if abs(v2)>=1E8
        break
    end
    % the next line is used to find the appropriate velocity and acceleration
    % at the next time step as the procedure described in the verlet
    % velocity scheme assumes that the force (thereby acceleration) is not
    % dependent on velocity. However, as they are dependent on each other,
    % i used a root finder on the function Residual. Residual is described
    % below.
    acc(i+1)=V(t(i+1),x(i+1),v(i),m,c,k1,k3,A,w);
    v(i+1)=v2+0.5*acc(i+1)*dt;
end
end

```

A.1.5. RK4 scheme to numerically solve cases

```

function [t,x,v]=M475RK4(a,b,N,m,c,k1,k3,A,w,x0,v0)
dt=(b-a)/N;
x(1)=x0; %position
v(1)=v0; %velocity
t=a; %time

for i=1:N-1 % main loop, runge kutta
    kv1=dt*V(t(i),x(i),v(i),m,c,k1,k3,A,w);
    kx1=dt*v(i);
    kv2=dt*V(t(i)+0.5*dt,x(i)+0.5*kx1,v(i)+0.5*kv1,m,c,k1,k3,A,w);
    kx2=dt*(v(i)+0.5*kv1);
    kv3=dt*V(t(i)+0.5*dt,x(i)+0.5*kx2,v(i)+0.5*kv2,m,c,k1,k3,A,w);
    kx3=dt*(v(i)+0.5*kv2);
    kv4=dt*V(t(i)+dt,x(i)+kx3,v(i)+kv3,m,c,k1,k3,A,w);
    kx4=dt*(v(i)+kv3);
    t(i+1)=t(i)+dt;
    x(i+1)=(1/6)*(6*x(i)+kx1+2*kx2+2*kx3+kx4);
    v(i+1)=(1/6)*(6*v(i)+kv1+2*kv2+2*kv3+kv4);
end
end

```

A.1.6. Stable Steady-State Solution

```

function StableSSSolution(a,b,N,m,c,k1,k3,A,w,x0,v0)
close all
% nondimensional coefficients
zeta=c/(2*sqrt(m*k1));
kr=(k3*A^2)/k1^3;

omega=linspace(0,2,N);
% constants for equation 11
aa=(8/(3*kr)).*(1-omega.^2);
bb=(16/(9*kr^2)).*((1-omega.^2).^2+4*zeta^2.*omega.^2);
cc=-(16/(9*kr^2));

% discriminant, not needed unless to check if the system can be
% approximated with this scheme
%dis=4*aa^3*c-aa^2*bb^2-18*aa*bb*cc+4*bb^3+27*cc^3;
psi=acos((-aa.^3+(9/2).*aa.*bb-(27/2)*cc)./((aa.^2-3*bb).^(1.5)));

% root of equation 11
Y2=(1/3).*(-aa+2.*(aa.^2-3*bb).^(.5).*cos((1/3).*(psi+2*pi)));
X02=sqrt(Y2);

%% plotting Nondimensional graph
plot(omega,real(X02),'r');
title(sprintf('Nondimensionalize Amplitude\nVersus Frequency Ratio'));
hold on
%plot(omega,imag(X02),'b');
text(0,max(real(X02),[],2),sprintf('Zeta = %.2f\nkr = %.2f',zeta,kr));
xlabel('$\Omega$', 'Interpreter', 'latex')
ylabel('$X_0$', 'Interpreter', 'latex')
legend('Real Part', 'Imaginary')

pause
%% plotting jump
close all
wm=omega(find(real(X02)==max(real(X02),[],2)))
max(real(X02),[],2)
[t,x,v]=M475VerletVelocity(a,b,N,m,c,k1,k3,A,wm,x0,v0);

subplot(2,1,1)

plot(t,x,'r')
title('Behavior at Peak Amplitude Ratio')
xlabel('t')
ylabel('X')
ylim([min(x,[],2) max(x,[],2)])
subplot(2,1,2)
if k3>0
    factor=1.01;
else
    factor=.99;
end

[t2,x2,v2]=M475VerletVelocity(a,b,N,m,c,k1,k3,A,wm*factor,x0,v0);
plot(t2,x2,'b')
title('1 Percent Movement of Frequency Ratio and Jump')
xlabel('t')
ylabel('X')
ylim([min(x,[],2) max(x,[],2)]);

```

```

%% plotting analyitcal solution
pause

close all
[t,x,v]=M475VerletVelocity(a,5*b,N*3,m,c,k1,k3,A,wm,x0,v0);
YM=(2/3)*(1-zeta^2)/(kr)*(-1+sqrt(1+(3*kr)/(4*zeta^2*(1-zeta^2))));
XM=sqrt(YM);
omegaM=sqrt(1-2*zeta^2+.75*kr*YM);
AnalSol=XM*cos(omegaM.*t);

plot(t(floor(N/3):end),x(floor(N/3):end),'r');
hold on
plot(t(floor(N/3):end),AnalSol(floor(N/3):end),'b');
xlabel('t');
ylabel('X');
title('Steady-State Analytical Solution');
legend('Numerical','Analytical');

end

```

A.1.7. Code to display Phase Planes

```

function [x,y,u,v,y1,y2]=DirectionMap(a,b,N,m,c,k1,k3,A,w,x0,v0,xrange,vrange)
f = @(t,Y) [Y(2); (c*Y(2) - k1*Y(1) - k3*Y(1)*Y(1)*Y(1))/m];

%Constructs mesh for direction field%
if xrange(1)==xrange(2)
    y1 = linspace(1,3,30);
else
    y1 = linspace(xrange(1),xrange(2),30);
end
if xrange(1)==xrange(2)
    y2 = linspace(-1,1,30);
else
    y2 = linspace(vrange(1),vrange(2),30);
end

[x,y] = meshgrid(y1,y2);

u = zeros(size(x));
v = zeros(size(y));
%Declaring time for the Driven system cases
t0=a;
dt=(b-a)/N;
tn=t0;
for i = 1:numel(x)
    Yprime = f(tn,[x(i); y(i)]);
    u(i) = Yprime(1);
    v(i) = Yprime(2);
    tn=t0+i*dt;
end
end

```